·数智神经外科学·

术中超声在脑肿瘤诊断与治疗中的应用

郭嘉禾　张晓磊　张恺

【摘要】 术中超声(iUS)是脑肿瘤手术中一种低成本、简便且易操作的辅助工具,但缺乏规范化操作指南。本文阐述iUS原理和应用流程、脑内病变超声可见度分级系统、iUS在脑肿瘤特别是胶质瘤切除评估中的应用效果和局限性、多模态超声成像及人工智能在iUS中的应用,多角度展示iUS在脑肿瘤手术中的应用,并提出实践规范。

【关键词】 脑肿瘤;　超声检查;　监测,手术中;　多模态成像;　综述

Clinical practice of intraoperative ultrasound in brain tumor surgery

GUO Jia-he, ZHANG Xiao-lei, ZHANG Kai

Department of Neurosurgery, Beijing Tsinghua Changgung Hospital, School of Clinical Medicine, Tsinghua Medicine, Tsinghua University, Beijing 102218, China

Corresponding author: ZHANG Kai (Email: zka04416@btch.edu.cn)

【Abstract】 Intraoperative ultrasound (iUS) is a low-cost, portable and user-friendly auxiliary tool in brain tumor surgery, yet there is a lack of standardized operational guidelines. This review begins with the ultrasound physics and summarizes the workflow of iUS, followed by a grading system for ultrasonographic visibility of intracerebral lesions, iUS in assessing brain tumor resection, the limitations of iUS-guided brain tumor resection, multimodal ultrasound imaging, and the application of artificial intelligence (AI) in iUS. This review shows the clinical practice of iUS in brain tumor surgery from multiple perspectives and proposes practical standards.

【Key words】 Brain neoplasms; Ultrasonography; Monitoring, intraoperative; Multimodal imaging; Review

This study was supported by Beijing Natural Science Foundation (No. L246048).

Conflicts of interest: none declared

实现脑肿瘤最大程度安全切除是神经外科手术追求的最终目标。术中MRI(iMRI)是目前术中评估肿瘤切除程度的“金标准”,但成本高,显著延长手术时间且需大量辅助人员,仅少数神经外科中心配备,不适宜临床推广。术中超声(iUS)操作便携,成本较低,易整合至常规手术流程中,是神经外科手术中常用的辅助设备之一,可用于辅助定位病灶、规划路径及评估切除范围。然而目前iUS操作者多为神经外科医师,大多未经超声科专业培训,且iUS缺乏规范化操作指南,给标准化实践带来困难。近年来,iUS在脑肿瘤临床诊断与治疗中的应用已有诸多更新,本文总结其新的应用范式,阐述iUS原理和应用流程、脑内病变超声可见度分级系统、iUS在脑肿瘤(特别是胶质瘤)切除评估中的应用和效果、多模态超声成像技术及人工智能(AI)技术在iUS中的应用,以为iUS的临床应用提供参考。

doi:10.3969/j.issn.1672-6731.2025.02.005

基金项目:北京市自然科学基金资助项目(项目编号:L246048)

作者单位:102218 清华大学附属北京清华长庚医院神经外科

通讯作者:张恺,Email:zka04416@btch.edu.cn

一、神经外科术中超声原理及应用流程

1.原理　神经外科iUS通常采用B型超声,通过向不同方向发射超声脉冲,接收相应回波信号,并将其幅度映射为辉度,获得切面回波图像信息。超声波反射发生于声阻抗变化的组织界面,声阻抗与组织弹性相关[1]。回波信号包含界面位置、形状、性状等信息,信号强度与回波信号振幅有关,振幅又与界面声学梯度呈正比,故声学梯度越大、振幅越大、回声越强。由于狭颅症患儿的术中全脑超声图像与标准解剖结构相似,故以狭颅症患儿为例展示术中全脑超声图像,颅骨呈明显强回声(图1a);

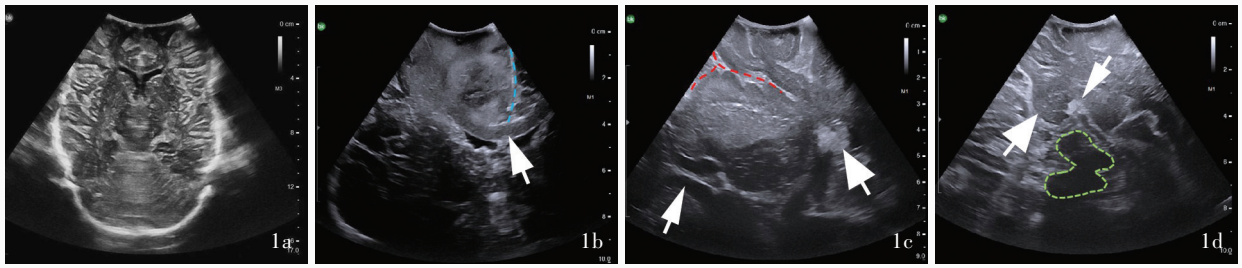

图1　脑部结构的iUS所见　1a　狭颅症患儿颅骨呈明显强回声　1b　*IDH*野生型胶质母细胞瘤患者纵裂及其周围结构可见肿瘤侵犯扣带回，内侧为高回声大脑镰（蓝色虚线所示），下方为胼胝体（箭头所示）　1c　Sturge-Weber综合征患者基底节呈等回声，基底节周围可见外侧岛叶结构和外侧裂（红色虚线所示），内侧可见低回声侧脑室（细箭头所示），后内侧可见低回声丘脑，脑室内可见高回声脉络丛（粗箭头所示）　1d　Sturge-Weber综合征患者颞叶内侧结构可见海马头（粗箭头所示）和海马体（细箭头所示），海马内侧可见低回声中脑（绿色虚线所示），中脑前方为鞍上池，海马头内侧与中脑之间可见大脑后动脉穿行

Figure 1　iUS findings of brain structures　The whole brain ultrasonography of a patient with craniostenosis. The skull exhibited pronounced hyperechoic characteristics (Panel 1a). Ultrasonography of longitudinal fissure and surrounding structures from a patient with *IDH*-wild type glioblastoma showed tumor invasion of the cingulate gyrus. Medially, the falx cerebri was hyperechoic (blue dotted lines indicate). The corpus callosum (arrow indicates) lay below it (Panel 1b). Ultrasonography of peri-basal ganglia structures from a patient with Sturge-Weber syndrome showed the basal ganglia with isoechoic signals, the lateral insular structures and the lateral sulcus (red dotted lines indicate). Medially, the hypoechoic lateral ventricle (thin arrow indicates) could be seen, with the hypoechoic thalamus located posteromedially. Hyperechoic choroid plexus (thick arrow indicates) was visible within the ventricle (Panel 1c). Ultrasonography of medial temporal lobe structures from the same patient with Sturge-Weber syndrome showed the hippocampal head (thick arrow indicates), the hippocampal body (thin arrow indicates), and the hypoechoic midbrain (at the level of the quadrigeminal plate, green dotted lines indicate) medial to the hippocampus. The suprasellar cistern was located anterior to the midbrain. The posterior cerebral artery traversed between the medial hippocampal head and the midbrain (Panel 1d).

通过观察不同疾病患者，发现高回声结构包括大脑镰（图1b）、脉络丛（图1c）、硬脑膜、血管壁、室管膜、脑组织-病灶界面，低回声结构包括结缔组织、脑室（图1c）、脑干（脑深部信号衰减，图1d），等回声结构为脑实质。除反射外，声能还可以通过能量吸收和折射发生衰减，声波频率越高、分辨率越佳，衰减程度越高。因此，高频探头适合浅表结构的精细成像，低频、低分辨率探头则适合脑深部结构的可视化并提供更大视野。

2.应用流程　神经外科iUS主要用于以下三方面[2]，一是实时定位病灶，了解其位置、边界和毗邻结构，甚至识别豆纹动脉[3]；二是规划脑深部病变入路[4]，特别是皮质下和颅底病变；三是术中实时评估病灶切除范围[5]。对于初学者，iUS的规范操作流程至关重要。（1）清洁与消毒：使用前须对所有设备进行清洁和消毒。若探头上体液或组织已干燥，消毒和灭菌处理可能无效，故使用后须立即严格遵守手术室管理制度，清洁探头上的凝胶和生物组织。此外，确诊或疑似克-雅病患者切勿使用iUS，一旦使用，须经医院审批程序销毁探头。由于部分探头套可能含有乳胶，建议术前明确患者是否对乳胶过敏并进行相应准备。（2）设备检查：术前常规检查iUS设备以保证其工作状态良好，包括探头、电缆、显示器及其他组件。根据手术部位和类型选择适宜探头，通过调整增益、时间增益补偿（TGC）、功率输出、帧率、动态范围等确保图像质量，并对捕获的超声图像进行分析。（3）探头选择：各类型探头参数不同，不同场景下应选择适宜探头，受限于骨窗大小，接触面积较小的探头更适合术中应用。多元换能器主要分为线阵、凸阵和凸面扇形阵探头，其中线阵和凸阵换能器接触面积较大，可分别用于体部血管肌肉成像（如BK Medical 18L5型探头，接触面积为63 mm×10 mm，频率5～18 MHz，扫描深度为2～9 cm）和腹部成像（如BK Medical 6C2型探头，接触面积69 mm×19 mm，频率2～6 MHz，扫描深度4～30 cm），在神经外科仅用于骨窗较大的开颅手术。上述探头频率较低，组织穿透性良好，扫描深度较深，可用于全脑超声成像（图2a），无导航超声时有助于建立标准扫描切面；接触面积较小的凸面扇形阵开颅探头（如BK Medical N13C5型探头，接触面积为29 mm×10 mm，频率5～13 MHz，扫描深度1～8 cm）和颅孔探头（如BK Medical N11C5s型探头，接触面积10.00 mm×8.60 mm，频率5～11 MHz，扫描深度0.50～11.00 cm）则常用于神经外科手术开颅成像（图2b）以及穿刺手术或颅孔成像（图2c）。Dixon等[1]总结各类型探头的优势和局限性，微凸面扇形阵探头和接触面积较小的“曲棍球”式线阵探头分别用于术前大视野成像和术腔残留病变成像。此外，用于经蝶手术的长探针式侧向辐射（side-firing）探头可以辅助垂体腺瘤[5]、颅咽管瘤[6]和斜坡脊索

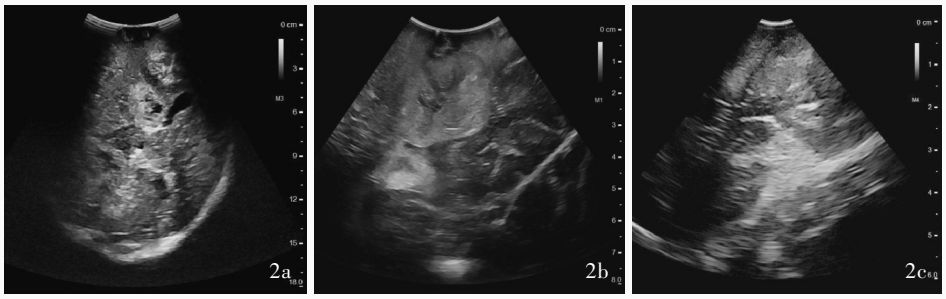

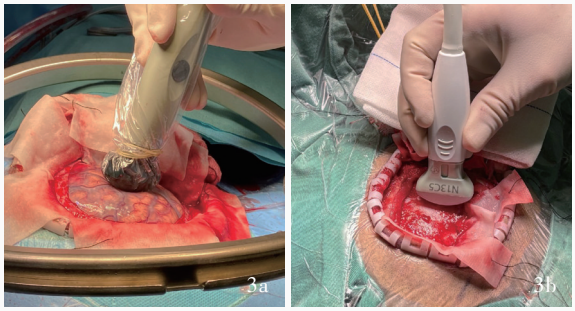

图2 超声探头选择 2a 具有毛细胞样特征的间变性星形细胞瘤采用BK Medical 6C2型探头进行全脑超声成像，频率3.50 MHz，增益4 dB，扫描深度18 cm 2b *IDH*突变型星形细胞瘤采用BK Medical N13C5型探头进行常规开颅成像，频率为8 MHz，增益为9 dB，扫描深度为8 cm 2c 弥漫性软脑膜胶质神经元肿瘤采用BK Medical N11C5s型探头进行小骨瓣开窗成像，频率为8 MHz，增益-3 dB，扫描深度6 cm **图3** 超声探头准备 3a 带有无菌覆膜套的探头 3b 灭菌探头

Figure 2 Ultrasound probe selection BK Medical 6C2 probe was used for a whole brain ultrasonography of anaplastic astrocytoma with pilocytic features. The imaging depth was 18 cm, with a frequency of 3.50 MHz and a gain of 4 dB (Panel 2a). BK Medical N13C5 probe was used for a conventional craniotomy ultrasonography of *IDH*-mutant astrocytoma. The imaging depth was 8 cm, with a frequency of 8 MHz and a gain of 9 dB (Panel 2b). BK Medical N11C5s probe was used for burr hole ultrasonography of diffuse leptomeningeal glioneuronal tumor. The imaging depth was 6 cm, with a frequency of 8 MHz and a gain of -3 dB (Panel 2c). **Figure 3** Ultrasound probe preparation Aseptic cover (Panel 3a). Sterilized ultrasound probe (Panel 3b).

瘤[7]的切除，并探查神经垂体[8]。临床应用时应根据目的采用不同的探头组合互补其优势和局限性。(4)探头准备：检查探头套与探头之间是否存在气泡并抚平，在探头顶端涂无菌凝胶或在探头套中加1～2 ml无菌生理盐水(图3a)，避免气泡产生的伪影，改进图像质量；可灭菌探头于灭菌后直接接触使用(图3b)，使用过程中应保持探头表面覆有无菌生理盐水，以保证图像质量并减少探头滑动扫描时对组织的损伤。(5)扫描方向：遵循标准化超声扫描方向十分重要，目标是获得与MRI相同的标准扫描平面(冠状位、矢状位、横断面)超声图像并进行对比观察。额部开颅手术应采取冠状位和矢状位，颞部开颅手术应采取冠状位和横断面，枕部和后颅窝开颅手术应采取横断面和矢状位[1,9-10]。(6)扫描流程：常规开颅手术将探头置于硬脑膜/蛛网膜表面，以无菌生理盐水为耦合剂，参照上述标准扫描方向进行多向滑动扫描，动作轻柔，反复以无菌生理盐水冲洗脑表面，减少机械摩擦损伤，录屏或截图并测量肿瘤大小；探查到病灶后确定位置，观察病灶形状、大小、内部回声(实性、囊性或混合性，是否均一)、边界与周围组织关系，以及正常脑室结构之间关系等；手术显微镜下切除病灶，从术腔取出棉片和脑压板，切勿放置明胶海绵或可吸收止血纱，以避免严重的后方伪影而无法评估残留病灶，填充无菌生理盐水；探头置于术腔，扫描评估切除范围和程度，并引导切除残留病灶；术毕缝合硬脑膜，扫描评估缝合严密程度并检查是否有活动性出血。随着手术器材、止血技术的提高以及术后6 h内CT检查的应用，术后即刻超声扫描的获益不明显，Policicchio等[2]报告163例iUS评估颅内病变患者，仅2例发生术后出血，其中iUS检出1例。

二、脑内病变超声可见度分级系统

2013年，Mair等[11]根据超声显示的整体病灶可见度和边界对脑内病变进行超声可见度分级，尽管与其他分级系统类似[12-13]，但该分级系统描述全面、接受度最广，共分为4级(表1[11]，图4～6)，涵盖脑肿瘤、脑脓肿、脑海绵状血管瘤、颅内动静脉畸形、颅内血肿等21种病理类型共计105例脑内病变患者，其中3级占40%(42/105)、2级占52.38%(55/105)、1级占7.62%(8/105，包括低级别胶质瘤4例、颅内动静脉畸形2例、颅内肉芽肿和少突胶质细胞瘤各1例)。他们还发现，高级别胶质瘤、脑转移瘤、脑膜瘤、室管膜瘤和血管母细胞瘤的中位超声可见度分级≥2级，而低级别星形细胞瘤和少突胶质细胞瘤的中位超声可见度分级≤2级[11]。2018年，Policicchio等[2]纳入163例脑肿瘤、脑血管病和颅内感染性病变患者，重新评估该分级系统的应用，发现除1例颅内动脉瘤(超声可见度分级0级)外，余162例均为超声可见度分级1～3级；与轴内肿瘤相比，脑膜瘤、神经鞘瘤和颅咽管瘤等轴外肿瘤更易辨别且边界更清晰；与胶质瘤相比，脑转移瘤更易辨别；与低级别胶质瘤相比，高级别胶质瘤更易辨

表1　脑内病变超声可见度分级系统[11]

Table 1.　A practical grading system of ultrasonographic visibility for intracerebral lesions[11]

分级	可见度	边界	描述
0级	不可见	不可见	病变不可见
1级	差	差	病变难以辨别，与周围正常脑组织边界不清
2级	好	差	病变可辨别，与周围正常脑组织边界不清
3级	好	好	病变可辨别，与周围正常脑组织边界清晰

图4　儿童型弥漫性高级别胶质瘤，超声可见度分级1级，术前MRI和iUS所见　4a　横断面T_2WI显示，左侧颞叶肿胀，呈异常高信号，弥漫浸润性生长，无明显边界（箭头所示）　4b　iUS无法辨别肿瘤结构，病变难以辨别，与周围正常脑组织边界不清，为超声可见度分级1级（箭头所示）　4c　T_2-FLAIR成像（超声同层面、同视野）亦无法辨别肿瘤结构，病变难以辨别，与周围正常组织边界不清（箭头所示）

Figure 4　Preoperative MRI and iUS findings of pediatric-type diffuse high-grade glioma classified as ultrasonographic visibility Grade 1　Axial T_2WI showed the lesion as hyperintense with diffuse infiltrative growth and no clear boundaries in the left temporal lobe (arrow indicates, Panel 4a).　iUS (Panel 4b) and T_2-FLAIR in the same ultrasound field of view (Panel 4c) couldn't distinguish the tumor, making the lesion difficult to identify, with unclear boundaries from surrounding normal tissue, consistent with Grade 1 (arrows indicate).

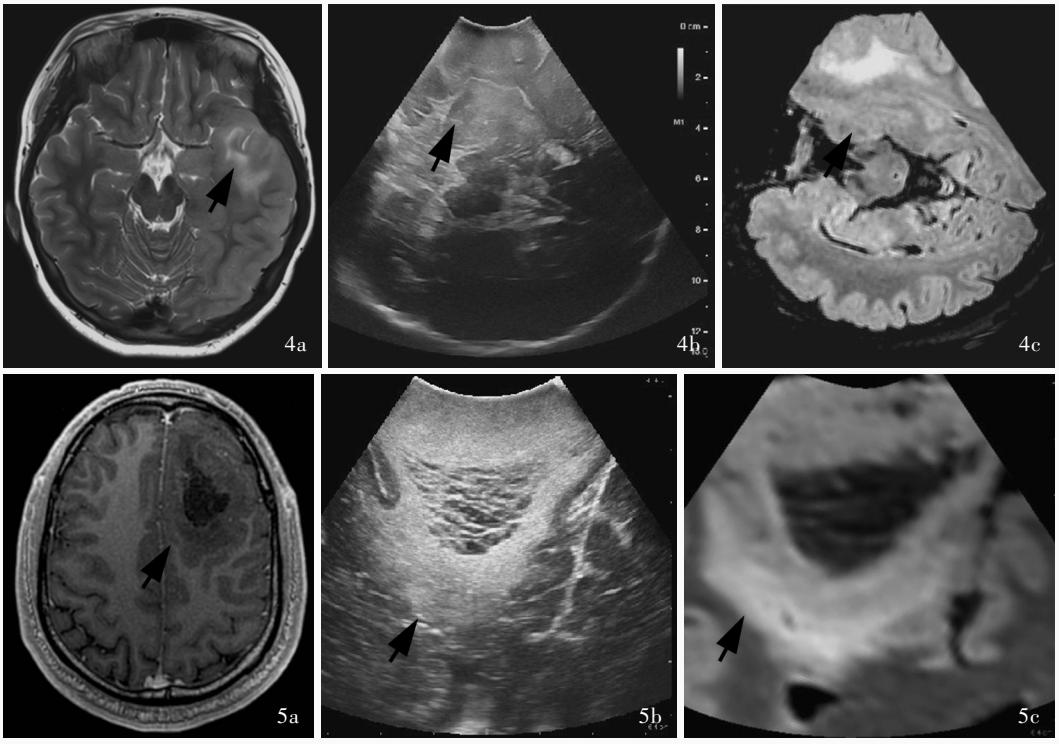

图5　*IDH*突变型星形细胞瘤（WHO 4级），超声可见度分级2级，术前MRI和iUS所见　5a　横断面增强T_1WI显示左侧额叶占位性病变，呈低信号，弥漫浸润性生长，呈轻度斑片样强化（箭头所示）　5b　iUS显示病变呈高回声，内部呈混杂回声，病变可辨别，与周围正常脑组织边界不清，为超声可见度分级2级（箭头所示）　5c　T_2-FLAIR成像（超声同层面、同视野）显示病变呈高信号，内部囊性变呈低信号（箭头所示）

Figure 5　Preoperative MRI and iUS findings of *IDH*-mutant astrocytoma (WHO grade 4) classified as ultrasonographic visibility Grade 2　Axial enhanced T_1WI showed the mass lesion as hypointense with patchy enhancement and diffuse infiltrative growth in the left frontal lobe (arrow indicates, Panel 5a).　iUS showed the tumor as hyperechoic with mixed echoes internally.　The lesion was discernible but has unclear boundaries with surrounding normal tissue, consistent with Grade 2 (arrow indicates, Panel 5b).　T_2-FLAIR in the same ultrasound field of view showed hyperintensity of the lesion and cystic changes appearing as hypointensity (arrow indicates, Panel 5c).

别。虽常可见轴内肿瘤（包括脑转移瘤）伪影导致的超声图像质量下降，而脑海绵状血管瘤、脑脓肿、颅内动静脉畸形和轴外肿瘤（脑膜瘤、鞍区肿瘤、神经鞘瘤）等非浸润性病变超声可见度分级无明显下降，但iUS对病变切除程度评估的精确性高于仅应用显微镜，故iUS仍然有意义。

三、术中超声在脑肿瘤切除评估中的作用

1. 评估方法　iMRI是术中评估病变切除程度的“金标准”，iUS因缺乏标准的解剖切面，难以对比切除程度，因此，采用iUS进行切除评估时不仅遵循标准化超声扫描流程，而且应选择适宜的评估方法。常规方法是将术前和术后影像学数据导入图像处理软件进行重建，勾画感兴趣区（ROI），计算术前和术后残留肿瘤体积，再计算切除程度。该方法在神经外科手术中被广泛应用，但需iMRI和辅助软件，耗时较长且无法实时引导。为实现简单实用的

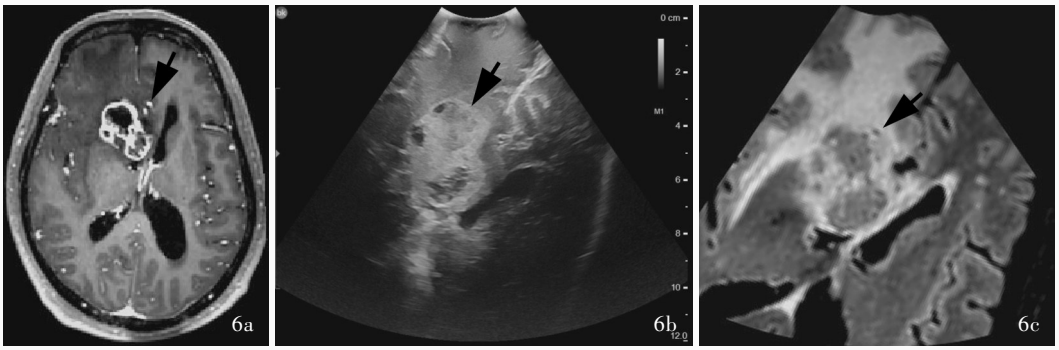

图6 具有毛细胞样特征的间变性星形细胞瘤，超声可见度分级3级，术前MRI和iUS所见 6a 横断面增强T_1WI显示右侧额叶占位性病变，呈明显强化，内部囊性变，伴周围指状低信号水肿带（箭头所示） 6b iUS显示病变呈明显强回声，可与周围水肿区分，内部呈低回声囊性变，病变可辨别，与周围正常脑组织边界清晰，为超声可见度分级3级（箭头所示） 6c T_2-FLAIR成像（超声同层面、同视野）显示病变呈混杂高或等信号，伴周围指状高信号水肿带（箭头所示）

Figure 6 Preoperative MRI and iUS findings of anaplastic astrocytoma with pilocytic features classified as ultrasonographic visibility Grade 3 Axial enhanced T_1WI showed significant enhancement of the lesion, with internal necrosis and surrounding hypointense edema in the right frontal lobe (arrow indicates, Panel 6a). iUS showed the tumor as markedly hyperechoic, distinguishable from surrounding edema, with hypoechoic cystic changes internally. The lesion was discernible with clear boundaries from surrounding normal tissue, consistent with Grade 3 (arrow indicates, Panel 6b). T_2-FLAIR in the same ultrasound field of view showed mixed hyperintensity-isointensity of the lesion, accompanied by surrounding hyperintense edema (arrow indicates, Panel 6c).

iUS切除程度评估，Aibar-Duran等[9]采用一种近似计算方法，即椭球体积公式（体积=4/3×π×A×B×C），通过二维超声进行两次正交图像采集，测量术前和术后残留肿瘤长径（A）、短径（B）和厚度（C），计算术前和术后残留肿瘤体积，再计算切除程度。该方法简便，与三维体积重建呈强正相关，可术中实时评估切除程度。

2.评估效果 轴外肿瘤超声可见度分级高且术中不易变化，适用于术中实时监测切除程度，如辅助切除垂体腺瘤[14]、脑转移瘤[15]和内镜下切除深部镰旁脑膜瘤[16]，但多数轴外肿瘤与周围脑组织边界明显或存在假边界，易于直视下切除，且颅底骨性结构限制iUS的应用，因此，iUS在轴外肿瘤手术中的应用较少。轴内肿瘤（特别是胶质瘤）边界不清，低级别胶质瘤超声可见度分级低且术中易变化，iUS可显著提高弥漫性胶质瘤切除程度[17]，并提高全切除（GTR）率[18]。多项Meta分析显示，与传统导航相比，iUS可延长高级别胶质瘤患者总生存期（OS）和提高全切除率[19-20]。复发性胶质瘤应用iUS，可使残留肿瘤体积更小，增加Karnofsky功能状态评分（KPS），延长复发间隔时间[21]。儿童低级别胶质瘤应用iUS，可以显著提高肿瘤全切除率，并降低复发率[22]。但对于脑深部肿瘤如幕上中线肿瘤，iMRI在残留肿瘤的可视化方面优于iUS[23]。

3.导航超声在切除程度评估中的应用 导航超声可实时监测脑肿瘤切除程度并计算残留肿瘤体积[9]。大多数神经外科中心的术中导航均基于术前影像学数据，而术中脑组织相对位置可随手术操作和脑脊液流失发生动态变化，即脑漂移，因此为保持术中导航的实时性，需动态更新导航图像。iMRI是导航图像更新的“金标准”，但成本高，临床应用受限。导航超声的核心是超声图像校准，将术前或术中影像学数据“注册”到同一空间，既可实时更新，又可获得iUS与术前MRI的对应关系，其本质为体积超声数据，通过整合二维超声图像实现三维成像。与二维超声相比，导航超声可更好地指导胶质瘤切除，提高全切除率[24]，优于仅应用神经导航[18]，还可以评估胶质瘤和脑转移瘤切除程度，校正脑脊液流失引起的脑漂移[25]。神经外科医师应用导航超声与神经放射科医师应用术后MRI评估切除程度的一致性较高，故导航超声纳入手术工作流程既安全又高效[26]。此外，导航超声结合微型腔内探头有助于消除超声伪影并实现预期的皮质下纤维束保护[27]。导航超声可以克服二维超声的限制，融合超声及其他多模态MRI图像，不同图像之间互补，是目前神经外科手术的重要工具。

4.术中超声引导脑肿瘤切除的局限性 iUS最重要的局限性是各种伪影导致的图像质量下降且难以解释。Toma等[28]在岛叶胶质瘤手术中发现，岛叶内侧MRI正常区域的iUS表现为岛叶内侧肿瘤边界明显高回声，分析其原因可能是岛叶内侧灰质与白质交替排列的正常结构，但iUS可能误认为肿

瘤而切除，引起严重的术后神经功能缺损。肿瘤切除后伪影使图像评估更复杂且难以解释，特别是体位摆放导致手术通道无法垂直于地面时，生理盐水无法充满术腔，滞留的空气可能导致明显低回声伪影，称为声真空（acoustic vacuum），即声波传播过程中遇到极低（如空气）或极高（如骨骼）声阻抗结构时被完全反射，界面产生强回声，声波无法穿过该界面，形成界面后阴影锥。声真空极易被经验较少的青年医师误认为是手术切除的残腔，从而提前结束手术[27]。

四、多模态超声成像

B型超声是iUS最广泛应用的模态，随着超声技术的进步，弹性超声成像、增强超声成像（CEUS）和多普勒超声成像等多模态超声成像也应用于iUS，用于鉴别肿瘤类型，评估肿瘤周围结构和肿瘤切除程度等[1]。

1.弹性超声成像　神经外科医师常在打开颅骨或硬脑膜后通过手动触诊感受组织可压缩性和刚度的固有差异，以区分肿瘤与周围脑组织[29]。弹性超声成像通过测量组织刚度（即杨氏模量），计算应力（施加的机械力）与应变（成比例变形）之间的关系，评估其病理状态[30-31]。组织回声主要与声阻抗相关，而与组织刚度通常不相关，弹性超声成像可提供额外信息辅助区分组织，尤以应变弹性成像（SE）和剪切波弹性成像（SWE）应用最为广泛。应变弹性成像是定性弹性评估技术，通过探头对脑实质施加轻微压力，测量其相对于正常邻近脑组织的变形量[32-33]，可用于测量肿瘤体积，较B型超声更好地描绘肿瘤边界[33]。与正常脑组织和低级别胶质瘤不同，高级别胶质瘤的肿瘤实质刚度较低且不均匀[32,34]。然而，应变弹性成像高度依赖操作者和超声设备，主观性较强，即使是硬件或软件的微小变化也可能导致图像明显改变，目前尚无相关成像标准，不同研究之间的测量值无法直接比较[35]。剪切波弹性成像是定量弹性评估技术，通过测量剪切波在组织中的传播速度定量评估组织刚度[30,36]，脑肿瘤实质刚度高于正常脑组织[37]，低级别胶质瘤亦高于高级别胶质瘤[38]。此外，剪切波弹性成像在检测残留肿瘤方面较神经外科医师的术中判断更为敏感[37]。与应变弹性成像相比，剪切波弹性成像可以提供肿瘤刚度的定量数据（绝对值），可重复性强。尽管取得上述进展，弹性超声成像的临床转化仍面临诸多挑战，包括操作者依赖、解释难度以及与组织学不确定性相关等[39]。

2.增强超声成像　欧洲医学和生物学超声学会联合会（EFSUMB）推荐，增强超声成像在神经外科手术中用于肿瘤识别、边界评估、灌注模式和残留肿瘤评估[40]。增强超声成像经静脉注射气体微泡，微泡呈高回声。部分轴内肿瘤边界不明确或重度脑水肿，超声可见度分级较低，B型超声难以评估肿瘤形态和边界，而增强超声成像的肿瘤边界可视化优于B型超声[41-44]，不仅突出显示肿瘤，还显示供血动脉和引流静脉以及微血管系统和灌注。轴内肿瘤与周围脑实质之间常有异常分布的毛细血管，增强超声成像可以显示肿瘤实质和肿瘤-脑组织界面，对比增强程度和分布与毛细血管密度相关。研究显示，高级别胶质瘤增强超声成像与术前MRI增强区域在形态和体积上密切相关[43]。增强模式和灌注定量分析有助于胶质瘤分级[45]，低级别胶质瘤轻度增强，边缘不清，灌注类似邻近正常脑组织；高级别胶质瘤在快速灌注和静脉引流的过程中伴血管紊乱，呈明显增强[41,46]。增强超声成像还有助于区分肿瘤与放射性坏死，后者无增强表现[47]。因此建议，打开硬脑膜前行增强超声成像，观察并测量其增强特征[48]；肿瘤切除前行增强超声成像，一方面提供基线肿瘤增强特征，便于术中重复测量；另一方面在高灌注区采样，这些高灌注区可能代表最高级别的肿瘤成分。若肿瘤表现为超声增强，建议切除后复查增强超声成像，确认残留肿瘤，其敏感性高于B型超声[45,49-50]。增强超声成像结合荧光素钠可以更好地识别肿瘤边界，辨别残留肿瘤并提高切除率[51]。增强超声成像辅助切除高级别胶质瘤可延长患者总生存期和无进展生存期（PFS）[51]。近年来，随着中枢神经系统肿瘤分子分型的提出，增强超声成像的研究集中于增强特征与肿瘤生物学行为和分子标志物的相关性[52-54]，其动态参数与多种病理学指标相关，可有效评估胶质瘤浸润程度[52]，检测异柠檬酸脱氢酶（*IDH*）突变状态[53-54]。

3.多普勒超声成像　多普勒超声成像原理主要与血管相关，在脑肿瘤中的应用较少，但iUS设备具备该功能，是最常用的超声成像模态之一。多普勒超声成像利用多普勒效应对血流进行成像和测量。彩色多普勒超声（CDUS）有助于评估肿瘤血供，并定位供血动脉和引流静脉。岛叶胶质瘤手术中医原性损伤豆纹动脉可导致严重偏瘫，Šteňo等[3,55]采用导航超声可视化豆纹动脉，降低豆纹动脉医原性损

伤风险。Della Pappa等[56]联合增强超声成像和彩色多普勒超声首次尝试术中直接栓塞血供丰富的血管母细胞瘤，实现术中出血可控并全切除肿瘤。除血管成像辅助外，多普勒超声成像还可以描述肿瘤灌注特征。Alafandi等[57]采用术中超快速多普勒超声观察成人型弥漫性胶质瘤的微血管特征，与MRI灌注特征相关。值得一提的是，功能超声成像是目前研究热点，其原理是超快速多普勒超声高时间和空间分辨率测量脑血容量的瞬时变化，可用于术中脑功能研究[58]。

五、人工智能在术中超声中的应用

人工智能推动医学影像学技术的发展，适用场景包括分类、检测和分割等任务，iUS也不例外。脑肿瘤图像分割任务推动医学图像分割领域多种算法的演进和应用，但目前多为MRI和CT等易获取的图像，分割算法在iUS图像中的应用很少，主要是由于超声数据较难收集和标准化程度较低。同时，iUS图像的脑肿瘤分割也存在巨大挑战[59]，不同观察者之间差异较大，浸润性肿瘤边界不清，超声设备参数变化明显影响图像质量，iUS图像随手术而变化，加之多数操作者经验尚浅，均影响iUS图像的判读。因此，亟待开发术中实时且泛用性强的iUS图像分割工具以辅助脑肿瘤切除。

目前公开的脑肿瘤超声图像数据集主要包括ReMIND[60]和RESECT[61-62]，可提供MRI和iUS图像的多模态数据，用于验证模态间配准算法，以及开发其他图像处理方法如去噪和分割。Rahmani等[63]提出双判别器贝叶斯生成对抗网络（D2BGAN）对MRI-iUS数据进行自动无监督配准，进一步提高模态间配准准确率。Cepeda等[64-65]采用BraTioUS数据集开发用于iUS图像胶质瘤分割的卷积神经网络（CNN）模型，并在各种外部数据集甚至图像质量较低的数据集中验证其泛用性和可重复性，并提取iUS影像组学特征构建胶质母细胞瘤存活模型。为增强iUS在脑肿瘤识别中的可解释性，有研究者通过YOLO11架构训练脑肿瘤检测模型，并实现术中实时监测（待发表）。此外，人工智能还可以构建多模态数据之间的关联。分子病理学特征是胶质瘤诊断、分级和治疗的关键因素，而病理学检查结果通常于肿瘤切除后1～2周回报，限制分子病理学对手术的指导。实时获取的iUS图像在快速术中分子诊断方面独具优势。Xie等[66]采用超声射频信号和深度学习（DL）对胶质瘤进行快速术中分子诊断（*IDH*突变、*TERT*启动子突变和1p/19q共缺失），并进行前瞻性队列验证。基于深度学习的增强超声成像视频自动分析也可以实现胶质瘤手术中实时检测*IDH*突变状态[53]。

六、展望

1. 伪影消除　iUS的重要挑战是手术结束时肿瘤边界可能出现明显高回声伪影，即使应用生理盐水或乳酸林格液也难以消除脑深部伪影。Unsgård等[67]研发一种新的声学耦合流体，具有与正常脑组织或肿瘤组织相同的衰减效果，可以减少或消除伪影，但尚未广泛应用。目前亟待开发新的生物相容性超声耦合剂以及计算机算法辅助伪影消除，以更好地识别超声下脑结构并评估肿瘤切除程度。

2. 自动化超声图像残留肿瘤检测　残留肿瘤检测是影像学技术的主要术中应用，轴外肿瘤、脑转移瘤的超声可见度分级均较高，切除时存在边界或假边界，经验丰富的神经外科医师无需术中影像学技术辅助也可全切除肿瘤。但胶质瘤残留肿瘤检测存在挑战性，低级别胶质瘤的超声可见度分级显著低于高级别胶质瘤，难以通过iUS对肿瘤切除范围进行评估[68]，而且超声可见度分级随手术操作而下降，仅依赖视觉对超声图像进行分析已经无法满足临床需求，需开发自动化超声图像残留肿瘤检测工具，以提高脑肿瘤切除率。

3. 术中超声的标准化实践　iUS虽被认为是一种实用的脑肿瘤切除范围评估工具，且多项回顾性研究证实其临床实用性，但仍缺乏高级别循证医学证据。Fountain等[69]对实现胶质瘤最大安全切除的术中影像学技术进行系统综述，但并未纳入iUS相关文献。正在进行的FUTURE-GB（The Functional and UlTrasound gUided Resection of GlioBlastoma）试验旨在研究标准手术方案（神经导航和5-氨基乙酰丙酸）基础上扩散张量成像（DTI）和iUS对胶质母细胞瘤患者无进展生存期的影响，从而决定iUS能否成为胶质母细胞瘤标准手术实践的一部分[70]。此外，高度规范应用超声设备方可最大限度发挥iUS的临床价值。iUS的学习曲线陡峭，如何进行相关人员培训也是规范超声设备应用的重要内容[71]。Weld等[72]将琼脂注射入离体动物脑组织以模拟脑肿瘤，构建真实且低成本模型，用于iUS研究和临床培训。术后常规分析iUS和MRI图像可提高对残留肿瘤的辨别能力，最大限度利用每例病例拉平该项技术的学习曲线[73]。

综上所述，极佳的声学特性使大脑成为超声波传播和图像生成的理想介质，但颅骨阻隔使得超声检查仅可在术中应用，但并不能阻碍神经外科医师应用超声的热情。越来越多的证据支持iUS评价肿瘤切除程度的实用性和可靠性，超声多模态特性可指导手术，实时提供脑肿瘤与周围脑组织的结构和功能信息。人工智能技术的发展改善iUS图像识别配准等多方面。尽管iUS存在诸如伪影等局限性，但其在实时引导和评估肿瘤切除程度方面的潜力，使其成为脑肿瘤手术中不可或缺的重要工具。随着神经外科iUS操作的规范，iUS有望成为脑肿瘤手术的标准流程，改善患者手术结局。

志谢 感谢山东大学附属儿童医院神经外科王广宇主任提供的狭颅症患儿术中全脑超声图像

利益冲突 无

参 考 文 献

[1] Dixon L, Lim A, Grech-Sollars M, Nandi D, Camp S. Intraoperative ultrasound in brain tumor surgery: a review and implementation guide[J]. Neurosurg Rev, 2022, 45:2503-2515.

[2] Policicchio D, Doda A, Sgaramella E, Ticca S, Veneziani Santonio F, Boccaletti R. Ultrasound-guided brain surgery: echographic visibility of different pathologies and surgical applications in neurosurgical routine [J]. Acta Neurochir (Wien), 2018, 160:1175-1185.

[3] Šteňo A, Buvala J, Toma D, Jezberová M, Šteňo J. Navigated 3D-ultrasound power Doppler and visualization of lenticulostriate arteries during resections of insular gliomas[J]. Brain Spine, 2022, 2:100873.

[4] García Pérez F, Vargas López AJ, Gomar Alba M, Velasco Albendea FJ, Guil Ibáñez JJ, Urreta Juárez G, Castelló Ruiz MJ, Narro Donate JM, Masegosa González J. Transcortical transcatheter ultrasound-assisted technique for deep-seated brain tumors: technical note[J]. J Ultrasound, 2024, 27:191-197.

[5] Mosallami Aghili SM, Maroufi SF, Sabahi M, Esmaeilzadeh M, Dabecco R, Adada B, Borghei-Razavi H. Intraoperative ultrasonography in pituitary surgery revisited: an institutional experience and systematic review on applications and considerations[J]. World Neurosurg, 2023, 176:149-158.

[6] Finger G, Wu KC, Godil SS, Carrau RL, Hardesty D, Prevedello DM. Ultrasound-guided endoscopic endonasal resection of sellar and suprasellar craniopharyngiomas[J]. Front Surg, 2023, 10:1073736.

[7] Baker KE, Robbins AC, Kumm ZT, Ziemke MK, Washington CW, Luzardo GD, Taylor CS, Stringer SP, Zachariah MA. Case report: side-firing intraoperative ultrasound guided endoscopic endonasal resection of a clival chordoma[J]. Front Oncol, 2023, 13:1039159.

[8] Juncker RB, Finger G, Damante MA, Prevedello LM, Prevedello DM, Wu KC. Real-time intraoperative ultrasound imaging of the posterior pituitary gland during endoscopic endonasal approach [J]. Acta Neurochir (Wien), 2024, 166:456.

[9] Aibar-Duran JA, Salgado-López L, Anka-Tugbiyele MO, Mirapeix RM, Gallardo Alcañiz A, Patino Alvarado JD, Rico Pereira M, Rodríguez Rodríguez R, Munoz-Hernandez F, de Quintana-Schmidt C. Navigated intraoperative ultrasound in neuro-oncology: volumetric accuracy and correlation with high-field MRI[J]. J Neurosurg, 2024, 141:79-88.

[10] Wu H, Cheng Y, Gao W, Chen P, Wei Y, Zhao H, Wang F. Progress in the application of ultrasound in glioma surgery[J]. Front Med (Lausanne), 2024, 11:1388728.

[11] Mair R, Heald J, Poeata I, Ivanov M. A practical grading system of ultrasonographic visibility for intracerebral lesions[J]. Acta Neurochir (Wien), 2013, 155:2293-2298.

[12] Shinoura N, Takahashi M, Yamada R. Delineation of brain tumor margins using intraoperative sononavigation: implications for tumor resection[J]. J Clin Ultrasound, 2006, 34:177-183.

[13] Solheim O, Selbekk T, Jakola AS, Unsgård G. Ultrasound-guided operations in unselected high-grade gliomas: overall results, impact of image quality and patient selection[J]. Acta Neurochir (Wien), 2010, 152:1873-1886.

[14] Baker KE, Robbins AC, Wasson RG, McCandless MG, Lirette ST, Kimball RJ, Washington CW, Luzardo GD, Stringer SP, Zachariah MA. Side-firing intraoperative ultrasound applied to resection of pituitary macroadenomas and giant adenomas: a single-center retrospective case-control study[J]. Front Oncol, 2022, 12:1043697.

[15] Di Cristofori A, Carone G, Rocca A, Rui CB, Trezza A, Carrabba G, Giussani C. Fluorescence and intraoperative ultrasound as surgical adjuncts for brain metastases resection: what do we know? A systematic review of the literature[J]. Cancers (Basel), 2023, 15:2047.

[16] Xiao J, Zhao T, Cheng X, Sheng Q, Li C, Li Y, Zhang Y, Wang X, Cheng H, Ye L. Transcranial resection of falcine meningiomas by complete endoscopy with the assistance of intraoperative ultrasound[J]. Neurosurg Rev, 2025, 48:21.

[17] Anichini G, Shah I, Mahoney DE, Patel N, Pakzad-Shahabi L, Da Costa OF, Syed N, Perryman R, Waldman A, O′Neill K. 3D ultrasound-augmented image guidance for surgery of high-grade gliomas: a quantitative analysis focused on the extent of resection[J]. Surg Neurol Int, 2024, 15:324.

[18] Guo X, Xing H, Pan H, Wang Y, Chen W, Wang H, Zhang X, Liu J, Xu N, Wang Y, Ma W. Neuronavigation combined with intraoperative ultrasound and intraoperative magnetic resonance imaging versus neuronavigation alone in diffuse glioma surgery [J]. World Neurosurg, 2024, 192:e355-e365.

[19] Palavani LB, Ferreira MY, Borges PGLB, Bandeira L, da Silva Semione G, Almeida MV, Verly G, Polverini AD, Andreão FF, Camerotte R, Ferreira CC, Paiva W, Bertani R, Boockvar J. Ultrasound-guided resection of high-grade gliomas: a single-arm meta-analysis[J]. World Neurosurg, 2024, 186:17-26.

[20] Pichardo-Rojas PS, Zarate C, Arguelles-Hernández J, Barrón-Lomelí A, Sanchez-Velez R, Hjeala-Varas A, Gutierrez-Herrera E, Tandon N, Esquenazi Y. Intraoperative ultrasound for surgical resection of high-grade glioma and glioblastoma: a meta-analysis of 732 patients[J]. Neurosurg Rev, 2024, 47:120.

[21] Wang M, Yu J, Zhang J, Pan Z, Chen J. Intraoperative ultrasound in recurrent gliomas surgery: impact on residual tumor volume and patient outcomes[J]. Front Oncol, 2023, 13:1161496.

[22] Klein Gunnewiek K, van Baarsen KM, Graus EHM, Brink WM, Lequin MH, Hoving EW. Navigated intraoperative ultrasound in pediatric brain tumors[J]. Childs Nerv Syst, 2024, 40:2697-2705.

[23] Dietvorst S, Narayan A, Agbor C, Hennigan D, Gorodezki D, Bianchi F, Mallucci C, Frassanito P, Padayachy L, Schuhmann MU. Role of intraoperative ultrasound and MRI to aid grade of

resection of pediatric low - grade gliomas: accumulated experience from 4 centers[J]. Childs Nerv Syst, 2024, 40:3165-3172.

[24] Moiyadi A, Shetty P, Singh VK, Yeole U. Intraoperative navigated three - dimensional ultrasound guidance improves resection in gliomas compared with standard two - dimensional ultrasound - results from a comparative cohort study[J]. World Neurosurg, 2023, 180:e233-e242.

[25] West TR, Mazurek MH, Perez NA, Razak SS, Gal ZT, McHugh JM, Choi BD, Nahed BV. Navigated intraoperative ultrasound offers effective and efficient real - time analysis of intracranial tumor resection and brain shift [J]. Oper Neurosurg (Hagerstown), 2025, 28:148-158.

[26] Šteňo A, Karlík M, Mendel P, Čík M, Šteňo J. Navigated three-dimensional intraoperative ultrasound-guided awake resection of low - grade glioma partially infiltrating optic radiation[J]. Acta Neurochir (Wien), 2012, 154:1255-1262.

[27] Šteňo A, Buvala J, Šteňo J. Large residual pilocytic astrocytoma after failed ultrasound - guided resection: intraoperative ultrasound limitations require special attention [J]. World Neurosurg, 2021, 150:140-143.

[28] Toma D, Buvala J, Šteňo A. Hyperechoic area under insular gliomas: a potentially hazardous intraoperative ultrasound artifact [J]. World Neurosurg, 2024, 182:e899-e904.

[29] Skambath I, Kren J, Kuppler P, Buschschlueter S, Bonsanto MM. An attempt to identify brain tumour tissue in neurosurgery by mechanical indentation measurements[J]. Acta Neurochir (Wien), 2024, 166:343.

[30] Albakr A, Ben - Israel D, Yang R, Kruger A, Alhothali W, Al Towim A, Lama S, Ajlan A, Riva-Cambrin J, Prada F, Al-Habib A, Sutherland GR. Ultrasound elastography in neurosurgery: current applications and future perspectives [J]. World Neurosurg, 2023, 170:195-205.

[31] Hersh AM, Weber - Levine C, Jiang K, Young L, Kerensky M, Routkevitch D, Tsehay Y, Perdomo - Pantoja A, Judy BF, Lubelski D, Theodore N, Manbachi A. Applications of elastography in operative neurosurgery: a systematic review[J]. J Clin Neurosci, 2022, 104:18-28.

[32] Gennari AG, Doniselli FM, Coley J, Grisoli M, Quaia E, Souchon R, Prada F, DiMeco F. Intraoperative comparison between strain elastography and preoperative magnetic resonance imaging features in high - grade gliomas using fusion imaging: a pilot study[J]. World Neurosurg, 2024, 192:e83-e89.

[33] Prada F, Del Bene M, Rampini A, Mattei L, Casali C, Vetrano IG, Gennari AG, Sdao S, Saini M, Sconfienza LM, DiMeco F. Intraoperative strain elastosonography in brain tumor surgery [J]. Oper Neurosurg (Hagerstown), 2019, 17:227-236.

[34] Cepeda S, Barrena C, Arrese I, Fernandez-Pérez G, Sarabia R. Intraoperative ultrasonographic elastography: a semi-quantitative analysis of brain tumor elasticity patterns and peritumoral region [J]. World Neurosurg, 2020, 135:e258-e270.

[35] Kumarapuram S, Yu R, Manchiraju P, Attard C, Escamilla J, Navin A, Khuroo M, Elmogazy O, Gupta G, Sun H, Roychowdhury S. Applying shear wave and magnetic resonance elastography to grade brain tumors: systematic review and meta-analysis[J]. World Neurosurg, 2023, 178:e147-e155.

[36] Taljanovic MS, Gimber LH, Becker GW, Latt LD, Klauser AS, Melville DM, Gao L, Witte RS. Shear-wave elastography: basic physics and musculoskeletal applications [J]. Radiographics, 2017, 37:855-870.

[37] Chan HW, Uff C, Chakraborty A, Dorward N, Bamber JC. Clinical application of shear wave elastography for assisting brain tumor resection[J]. Front Oncol, 2021, 11:619286.

[38] Chauvet D, Imbault M, Capelle L, Demene C, Mossad M, Karachi C, Boch AL, Gennisson JL, Tanter M. In vivo measurement of brain tumor elasticity using intraoperative shear wave elastography[J]. Ultraschall Med, 2016, 37:584-590.

[39] Selbekk T, Brekken R, Indergaard M, Solheim O, Unsgård G. Comparison of contrast in brightness mode and strain ultrasonography of glial brain tumours[J]. BMC Med Imaging, 2012, 12:11.

[40] Sidhu PS, Cantisani V, Dietrich CF, Gilja OH, Saftoiu A, Bartels E, Bertolotto M, Calliada F, Clevert DA, Cosgrove D, Deganello A, D'Onofrio M, Drudi FM, Freeman S, Harvey C, Jenssen C, Jung EM, Klauser AS, Lassau N, Meloni MF, Leen E, Nicolau C, Nolsoe C, Piscaglia F, Prada F, Prosch H, Radzina M, Savelli L, Weskott HP, Wijkstra H. The EFSUMB guidelines and recommendations for the clinical practice of contrast - enhanced ultrasound (CEUS) in non - hepatic applications: update 2017 (long version)[J]. Ultraschall Med, 2018, 39:e2-e44.

[41] Arlt F, Chalopin C, Müns A, Meixensberger J, Lindner D. Intraoperative 3D contrast - enhanced ultrasound (CEUS): a prospective study of 50 patients with brain tumours[J]. Acta Neurochir (Wien), 2016, 158:685-694.

[42] Prada F, Mattei L, Del Bene M, Aiani L, Saini M, Casali C, Filippini A, Legnani FG, Perin A, Saladino A, Vetrano IG, Solbiati L, Martegani A, DiMeco F. Intraoperative cerebral glioma characterization with contrast enhanced ultrasound[J]. Biomed Res Int, 2014:ID484261.

[43] Prada F, Vitale V, Del Bene M, Boffano C, Sconfienza LM, Pinzi V, Mauri G, Solbiati L, Sakas G, Kolev V, D'Incerti L, DiMeco F. Contrast - enhanced MR imaging versus contrast - enhanced US: a comparison in glioblastoma surgery by using intraoperative fusion imaging[J]. Radiology, 2017, 285:242-249.

[44] Tao AY, Chen X, Zhang LY, Chen Y, Cao D, Guo ZQ, Chen J. Application of intraoperative contrast - enhanced ultrasound in the resection of brain tumors[J]. Curr Med Sci, 2022, 42:169-176.

[45] Prada F, Perin A, Martegani A, Aiani L, Solbiati L, Lamperti M, Casali C, Legnani F, Mattei L, Saladino A, Saini M, DiMeco F. Intraoperative contrast - enhanced ultrasound for brain tumor surgery[J]. Neurosurgery, 2014, 74:542-552.

[46] Cheng LG, He W, Zhang HX, Song Q, Ning B, Li HZ, He Y, Lin S. Intraoperative contrast enhanced ultrasound evaluates the grade of glioma[J]. Biomed Res Int, 2016:ID2643862.

[47] Mattei L, Prada F, Marchetti M, Gaviani P, DiMeco F. Differentiating brain radionecrosis from tumour recurrence: a role for contrast - enhanced ultrasound [J]? Acta Neurochir (Wien), 2017, 159:2405-2408.

[48] Prada F, Vetrano IG, Gennari AG, Mauri G, Martegani A, Solbiati L, Sconfienza LM, Quaia E, Kearns KN, Kalani MYS, Park MS, DiMeco F, Dietrich C. How to perform intra-operative contrast-enhanced ultrasound of the brain: a WFUMB position paper[J]. Ultrasound Med Biol, 2021, 47:2006-2016.

[49] Della Pepa GM, Sabatino G, la Rocca G. "Enhancing vision" in high grade glioma surgery: a feasible integrated 5-ALA + CEUS protocol to improve radicality[J]. World Neurosurg, 2019, 129:401-403.

[50] Prada F, Bene MD, Fornaro R, Vetrano IG, Martegani A, Aiani L, Sconfienza LM, Mauri G, Solbiati L, Pollo B, DiMeco F. Identification of residual tumor with intraoperative contrast - enhanced ultrasound during glioblastoma resection [J]. Neurosurg Focus, 2016, 40:E7.

[51] Fang Q, Hou Q, Liu X, Ma L, Jiang G, He Z. Enhancing the extent of resection in glioma surgery through the integration of

intraoperative contrast-enhanced ultrasound and fluorescein sodium[J]. World Neurosurg, 2024, 186:e662-e672.
[52] Hu X, Zhang G, Xie R, Wang Y, Zhu Y, Ding H. Contrast-enhanced ultrasound can differentiate the level of glioma infiltration and correlate it with biological behavior: a study based on local pathology[J]. J Ultrasound, 2024.[Epub ahead of print]
[53] Xie Y, Zhao C, Zhang X, Shen C, Qi Z, Tang Q, Guo W, Shi Z, Ding H, Yang B, Yu J. Intraoperative real-time IDH diagnosis for glioma based on automatic analysis of contrast-enhanced ultrasound video[J]. Ultrasound Med Biol, 2025, 51:484-493.
[54] Zhang X, Shi Z, Xie Y, Wang Y, Shen C, Qi Z, Zhang L, Yang B, Yu J, Ding H. Quantitative analysis using intraoperative contrast-enhanced ultrasound in adult-type diffuse gliomas with isocitrate dehydrogenase mutations: association between hemodynamics and molecular features[J]. Ultrasonography, 2023, 42:561-571.
[55] Šteňo A, Jezberová M, Hollý V, Timárová G, Šteňo J. Visualization of lenticulostriate arteries during insular low-grade glioma surgeries by navigated 3D ultrasound power Doppler: technical note[J]. J Neurosurg, 2016, 125:1016-1023.
[56] Della Pappa GM, Marchese E, Pedicelli A, Olivi A, Ricciardi L, Rapisarda A, Skrap B, Sabatino G, La Rocca G. Contrast-enhanced ultrasonography and color Doppler: guided intraoperative embolization of intracranial highly vascularized tumors[J]. World Neurosurg, 2019, 128:547-555.
[57] Alafandi A, Tbalvandany SS, Arzanforoosh F, van Der Voort SR, Incekara F, Verhoef L, Warnert EAH, Kruizinga P, Smits M. Probing the glioma microvasculature: a case series of the comparison between perfusion MRI and intraoperative high-frame-rate ultrafast Doppler ultrasound[J]. Eur Radiol Exp, 2024, 8:13.
[58] Imbault M, Chauvet D, Gennisson JL, Capelle L, Tanter M. Intraoperative functional ultrasound imaging of human brain activity[J]. Sci Rep, 2017, 7:7304.
[59] Weld A, Dixon L, Anichini G, Patel N, Nimer A, Dyck M, O′Neill K, Lim A, Giannarou S, Camp S. Challenges with segmenting intraoperative ultrasound for brain tumours[J]. Acta Neurochir (Wien), 2024, 166:317.
[60] Juvekar P, Dorent R, Kögl F, Torio E, Barr C, Rigolo L, Galvin C, Jowkar N, Kazi A, Haouchine N, Cheema H, Navab N, Pieper S, Wells WM, Bi WL, Golby A, Frisken S, Kapur T. ReMIND: the brain resection multimodal imaging database[J]. Sci Data, 2024, 11:494.
[61] Xiao Y, Fortin M, Unsgård G, Rivaz H, Reinertsen I. REtroSpective Evaluation of Cerebral Tumors (RESECT): a clinical database of pre-operative MRI and intra-operative ultrasound in low-grade glioma surgeries[J]. Med Phys, 2017, 44:3875-3882.
[62] Behboodi B, Carton FX, Chabanas M, de Ribaupierre S, Solheim O, Munkvold BKR, Rivaz H, Xiao Y, Reinertsen I. Open access segmentations of intraoperative brain tumor ultrasound images[J]. Med Phys, 2024, 51:6525-6532.
[63] Rahmani M, Moghaddasi H, Pour-Rashidi A, Ahmadian A, Najafzadeh E, Farnia P. D^{2}BGAN: dual discriminator bayesian generative adversarial network for deformable MR-ultrasound registration applied to brain shift compensation[J]. Diagnostics (Basel), 2024, 14:1319.
[64] Cepeda S, Esteban-Sinovas O, Singh V, Shetty P, Moiyadi A, Dixon L, Weld A, Anichini G, Giannarou S, Camp S, Zemmoura I, Giammalva GR, Del Bene M, Barbotti A, DiMeco F, West TR, Nahed BV, Romero R, Arrese I, Hornero R, Sarabia R. Deep learning-based glioma segmentation of 2D intraoperative ultrasound images: a multicenter study using the Brain Tumor Intraoperative Ultrasound Database (BraTioUS)[J]. Cancers (Basel), 2025, 17:315.
[65] Cepeda S, Esteban-Sinovas O, Singh V, Moiyadi A, Zemmoura I, Del Bene M, Barbotti A, DiMeco F, West TR, Nahed BV, Giammalva GR, Arrese I, Sarabia R. Prognostic modeling of overall survival in glioblastoma using radiomic features derived from intraoperative ultrasound: a multi-institutional study[J]. Cancers (Basel), 2025, 17:280.
[66] Xie X, Shen C, Zhang X, Wu G, Yang B, Qi Z, Tang Q, Wang Y, Ding H, Shi Z, Yu J. Rapid intraoperative multi-molecular diagnosis of glioma with ultrasound radio frequency signals and deep learning[J]. EBioMedicine, 2023, 98:104899.
[67] Unsgård G, Sagberg LM, Müller S, Selbekk T. A new acoustic coupling fluid with ability to reduce ultrasound imaging artefacts in brain tumour surgery: a phase Ⅰ study[J]. Acta Neurochir (Wien), 2019, 161:1475-1486.
[68] Bø HK, Solheim O, Kvistad KA, Berntsen EM, Torp SH, Skjulsvik AJ, Reinertsen I, Iversen DH, Unsgård G, Jakola AS. Intraoperative 3D ultrasound-guided resection of diffuse low-grade gliomas: radiological and clinical results[J]. J Neurosurg, 2019, 132:518-529.
[69] Fountain DM, Bryant A, Barone DG, Waqar M, Hart MG, Bulbeck H, Kernohan A, Watts C, Jenkinson MD. Intraoperative imaging technology to maximise extent of resection for glioma: a network meta-analysis[J]. Cochrane Database Syst Rev, 2021, 1:CD013630.
[70] Plaha P, Camp S, Cook J, McCulloch P, Voets N, Ma R, Taphoorn MJB, Dirven L, Grech-Sollars M, Watts C, Bulbeck H, Jenkinson MD, Williams M, Lim A, Dixon L, Price SJ, Ashkan K, Apostolopoulos V, Barber VS, Taylor A; FUTURE-GB Collaborators; Nandi D. FUTURE-GB: functional and ultrasound-guided resection of glioblastoma. A two-stage randomised control trial[J]. BMJ Open, 2022, 12:e064823.
[71] Yeole U, Singh V, Mishra A, Shaikh S, Shetty P, Moiyadi A. Navigated intraoperative ultrasonography for brain tumors: a pictorial essay on the technique, its utility, and its benefits in neuro-oncology[J]. Ultrasonography, 2020, 39:394-406.
[72] Weld A, Dixon L, Anichini G, Faoro G, Menciassi A, Camp S, Giannarou S. A method for mimicking tumour tissue in brain ex-vivo ultrasound for research application and clinical training[J]. Acta Neurochir (Wien), 2025, 167:13.
[73] Brugada-Bellsolà F, Rodríguez PT, González-Crespo A, Menéndez-Girón S, Panisello CH, Garcia-Armengol R, Alonso CJD. Intraoperative ultrasound and magnetic resonance comparative analysis in brain tumor surgery: a valuable tool to flatten ultrasound′s learning curve[J]. Acta Neurochir (Wien), 2024, 166:337.

（收稿日期：2025-01-20）
（本文编辑：吴春蕊）